Z. Phys. C - Particles and Fields 17, 69–84 (1983)

Zeitschrift für Physik C Particles and Fields

Improved Description of the Small-x Limit of Deep Inelastic Scattering

Marcelo Loewe[1]

II. Institut für Theoretische Physik der Universität Hamburg, D-2000 Hamburg, Federal Republic of Germany

Received 28 September 1982

Abstract. In this paper we attempt to find, within the framework of perturbative QCD, an improved description of the small-x region of deep-inelastic scattering. Motivated by results on the Pomeron in QCD, we investigate diagrams with a system of an arbitrary number of gluon lines in the t-channel. The gluon lines are allowed to interact pairwise in all possible combinations. We find that the leading behaviour of these diagrams comes from configurations where the gluon lines arrange themselves into non interacting, non-forward ladders. We then analyse couplings between gluon ladders, in particular non-planar ones. We compare our results with a previous study of Gribov, Levin, and Ryskin. In agreement with them we conclude that the sum of these diagrams leads to a tempered increase of the structure function in the small-x region.

I. Introduction

It is well-known that the standard approximation of perturbative QCD which nicely describes deep inelastic scattering in the Bjorken limit becomes inappropriate when the scaling variable x tends to zero. One might hope that by including more and more Feynman diagrams into the analysis, the perturbative description in the small-x region becomes better, although the limit $x \to 0$, is expected to require non perturbative effects. It is the aim of this paper to find an improved description within perturbative QCD.

A leading logarithmic analysis in the axial gauge [1, 2] shows us that the relevant Feynman diagram for the structure function in the small-x case, but x not too small, corresponds to a forward gluon ladder, more precisely to the discontinuity of a gluon ladder which begins at a valence quark and ends with a quark loop, that interacts with the external photon. The virtualities of the partons along the ladder are strongly ordered when going from the valence quarks to the photon. In the limit $x \to 0$ this diagram, however, leads to an answer for the structure function which violates the Froissart bound. This means that the naive single ladder approximation is not sufficient, and, therefore, it is mandatory to include another type of diagrams which could be relevant in the small-x region. The motivation for the choice of these diagrams in the hard regime comes from the Regge limit [3].

We know that at the level of a single ladder, the hard regime in the small-x region and the Regge limit are intimately connected. By studying the Pomeron kernel of the Regge limit in the regime of high transverse momenta, Dokshitzer [1] has shown that this kernel turns into the small-x kernel in Bjorken's regime.

In the Regge limit it is known [3] that diagrams with only two gluon lines in the t-channel violate the unitarity bound. In order to improve this behaviour we have to take into account diagrams with more gluon lines in the t-channel. This fact motivates us to study, now in the hard regime, diagrams with n gluon lines. Following the Regge limit analysis, we allow these gluon lines to interact in pairs, by exchanging gluons, in all possible ways as it is shown in Fig. 1.

The full system of n gluon lines has to be in the forward direction in order to contribute to the structure function. Any subsystem, however, where two

1 On leave from Universidad Católica de Chile, Santiago, Chile Permanent address after 1-10-82. Facultad de Física, Pontificia Universidad Católica de Chile, Casilla 114-D Santiago Chile

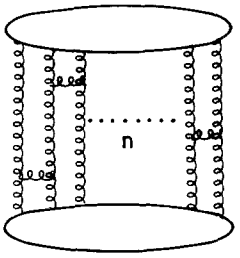

Fig. 1. A system of n gluon lines in the t-channel which can interact in pairs in all possible ways

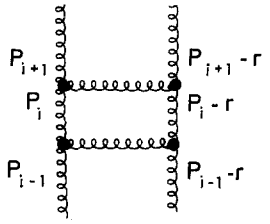

Fig. 2. The i^{th} cell in a non-forward gluon ladder

gluon lines interact corresponds to a non-forward cell. In a previous paper [4] we have studied the properties of non-forward gluon ladders in the hard regime for the small-x case. The i^{th} cell of such a ladder is shown in Fig. 2. In this paper we want to use the properties of the non-forward ladders to analyse the more complicated diagrams shown in Fig. 1.

Our analysis will enable us to conclude that in the hard regime, the maximum enhancement for such a class of Feynman diagrams corresponds to a configuration of non interacting non-forward ladders. Any possible gluon exchange between the ladders diminishes the enhancement of the amplitude. Moreover configurations with an odd number of gluon lines are not significant. These gluon ladders, as we will explain later, can be in planar or non-planar configurations.

It is important to study this system of interacting gluon lines also from another point of view, namely starting from the Regge limit. If we use the Pomeron kernel (without trajectories) in the regime of high transverse momenta, we get, as we should, an agreement with the above result. This consistency check is necessary in order to understand the transition from hard scattering (in the small-x limit) to Regge physics. On the other hand, if we include the trajectories we find some regions of the phase space where the interaction between the gluon ladders cannot be neglected. This new transverse enhancement, however, is sensitive to the infrared region and comes directly from the trajectories. As we know the trajectories are not present in the hard regime. These terms, therefore, signal the beginning of Regge physics.

Having decided in which configuration t-channel states of n gluons contribute to the structure function, it is necessary to study transitions from n gluon states to m gluon states and to decide how these configurations couple to valence quarks inside the hadron and to the photon at the upper end of the diagram. As to the transition: n gluons$\to m$ gluons $(m<n)$ we find that the dominant vertex is the combination of two gluon ladders into a single one. It could also be possible to have vertices where, in general, three or more ladders come together producing a smaller number of ladders. We will argue that such possibilities are not important. The ladders have to recombine in steps. At each step two ladders come together producing a single ladder. The vertex: 2 gluon ladders$\to$1 ladder is studied in detail. In particular we show that the non-planar vertex, in the relevant region of phase space, has the same form as the planar one. A space-time argument, however, indicates that the non-planar vertex is more likely than the planar one. The vertex where two ladders recombine into a single ladder enables us to go to smaller-x values. As we will see, the vertex does not belong to the leading logarithmic approximation because it behaves like $\frac{\alpha_s(|k_\perp|^2)}{|k_\perp|^2}$, where α_s is the usual running coupling constant. We can compensate the decreasing factor $\frac{\alpha_s(|k_\perp|^2)}{|k_\perp|^2}$ by taking smaller-x values which leave a longitudinal enhancement.

We then study the maximal non-planar loop (multiladder) diagram with two ladders, introducing a non-planar branching vertex, where a ladder branches into two ladders. We conclude that in the relevant diagram the number of gluon lines cannot increase while going from the valence quark up to the external photon. The non-forward ladders couple directly to the valence quarks.

Finally it is necessary to take the discontinuity of the full diagram and there are several possibilities how to choose the cuts of the amplitude. At this point an analysis of the validity of the AGK rules [5] turns out to be essential. We show for the non-planar vertex of two ladders, that the AGK rules are, in fact, valid. This rather technical point, which will be discussed in detail, turns out to by very important in order to get an alternating series for the summation of the relevant diagrams. Otherwise we cannot justify the convergence of the sum of infinitely many diagrams.

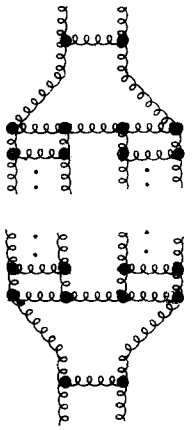

Fig. 3. An example of a planar multiladder diagram. This diagram is not relevant

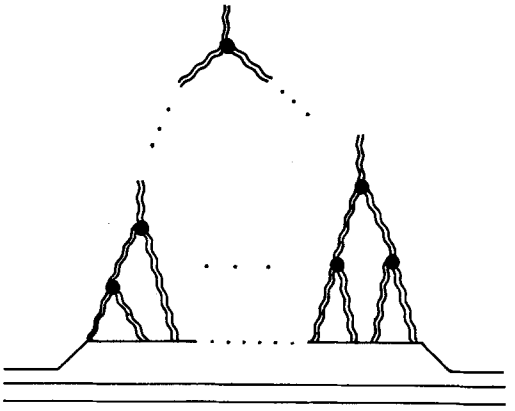

Fig. 4. The most general multiladder "fan" diagram. The wavy lines represent gluon ladders, and the points correspond to vertices where two ladders come together producing a single ladder

The idea of introducing diagrams with more gluons in the t-channel has first been considered by Gribov, Levin, and Ryskin [6, 7] (GLR). These authors have investigated what they call multiladder diagrams. The simplest example of a multiladder diagram is shown in Fig. 3. Here we have a loop of two independent gluon ladders in a planar configuration. It is clear that these ladders are non-forward ladders, and we have to integrate over the momentum which flows through the ladders. The choice of these diagrams: independent ladders which do not interact by means of gluon exchanges, apart from the lower branching vertex and the upper coupling where the ladders come together producing a single ladder, was not justified by GLR. We can understand this point from our previous discussion.

By studying the planar diagram of Fig. 3, GLR then showed that it will be relevant if there is no single ladder underneath the loop consisting of the two non-forward ladders. This means that the non-forward ladders must couple directly to the valence quarks. Such a diagram was called multiladder "fan" diagram and the upper ladder goes up to the external photon. It was found to be necessary that the momentum which flows through the ladders is kept small by hand, otherwise it destroys the possible enhancement of the diagram. As to the small-x behaviour, GLR found that this diagram violates the unitarity bound more strongly than the single ladder approximation. They, therefore, summed all possible "fan" diagrams getting an expression for the structure function consistent with unitarity in a well defined phase space region.

The most general "fan" diagram taken by GLR corresponds, if we start at the valence quarks, to a certain initial number of gluon ladders coming from the quarks. In the next step a pair of two ladders come together producing a single ladder which then combines with another ladder of the system in the same way. This is shown in Fig. 4 where the wavy lines represent gluon ladders. The number of gluon lines decreases when going to the external photon.

Compared to these results of GLR, our analysis provides an independent answer to the question, which diagrams should be summed in order to obtain a valid description of the small-x region. As to the general topology of the diagrams, we come to the same conclusion: t-channel states consisting of n gluons arrange themselves into non interacting gluon ladders, and when moving upwards from the valence quarks to the photon, the number of these ladders never increases. In more detail, however, we find that non-planar configurations are more important than the planar ones of GLR.

Since, nevertheless, the analytic form of the non-planar vertices coincides with the planar one (up to AGK rules and related questions of signs), the final conclusion of GLR remain valid. The infinite sum of all "fan" diagrams temper the small-x increase of the structure function, such that, in a well defined region of phase space, it is consistent with unitarity. This description is valid as long as x is larger than a certain function of Q^2:

$$\frac{8N}{b}\ln\frac{1}{x}<\frac{1}{4}e^{2\ln\ln\frac{Q^2}{\Lambda^2}},\qquad b=11-\frac{2}{3}n_f. \tag{1.1}$$

If x is smaller than this function, we have to take into account other contributions, and the above picture is not sufficient. Our argument which connects the small-x limit of the hard regime with the Regge limit indicates that other contributions which are infrared sensitive will come in. In fact, it is known [8] from unitarity that non perturbative effects have to enter.

It is important to note that the small x-region in e^+e^--physics has been treated in a different way. We know, since the work of Gribov and Lipatov [9], that at the leading logarithmic level the parton distributions in e^+e^- and deep inelastic scattering are the same. However, if we go beyond the leading approximation the parton distributions become different. In connection with the small x-case for e^+e^-, Mueller [10] was able to derive an expression for the anomalous dimension, by calculating up to three loops, which is no more divergent when $n\to 1$. Recently, Bassetto et al. [11] have confirmed this result by considering all the terms in the leading series of powers $g^2/(n-1)^2$. Such a calculation is not possible in the ep-case because the subdominant contributions present infrared problems.

This paper is organized as follows:

In Sect. II we analyse the system of n interacting gluon lines in the hard regime. Only independent ladders turn out to be important for the transverse enhancement of the amplitude.

Section III is devoted to a consistency check: we study the n gluon system starting from the Regge limit. We find agreement with the results of Sect. II.

In Sect. IV we study couplings between gluon ladders. In particular we analyse the non-planar coupling where two ladders come together producing a single ladder. We confirm the validity of the AGK rules and show that the maximal non-planar multiladder diagram with two ladders will be relevant only if there is no ladder underneath a loop consisting of two ladders, in agreement with GLR. The non-planar vertex also gives the same answer as the planar vertex. The main conclusions of this section can also be understood in a space time picture.

Finally in Sect. V we summarize our conclusions.

II. General Discussion of Diagrams with n Gluon Lines

In a previous paper [4] we have analysed QCD gluon ladder diagrams. This analysis was done in the axial gauge and applies to the small-x limit of the hard regime which is characterized by strong ordering of both the virtualities and longitudinal momenta. In what follows we will use the same techniques and notations of [4]. We briefely want to review here the attributes that characterize these ladder diagrams. For the details see [4].

a) The effective transverse kernel K for the i^{th} gluon cell Fig. 2 is given by:

$$K_\perp(p_i, p_i-r)=\frac{1}{|(p_i-r)_\perp|^2}+\frac{1}{|p_{i\perp}|^2}-\frac{|r_\perp|^2}{|(p_i-r)_\perp|^2|p_{i\perp}|^2}. \tag{2.1}$$

This kernel is regular for $p_{i\perp}\to 0$ and $p_{i\perp}=r_\perp$. In the above expression the denominators of the gluon propagators have been taken into account. In order to get the maximum number of logarithms coming from the transverse integrations, the $r_\perp$ component of the r momentum that flows through the ladder has to be as small as possible. In fact, $|r_\perp|^2$ gives us the lower bound for the set of transverse integrals.

b) The longitudinal kernel for the i^{th} gluon cell is given by:

$$K_l=\frac{\beta_{i-1}-\beta_i}{\beta_i(\beta_i-\beta_r)}. \tag{2.2}$$

We get the maximum small-x enhancement coming from the longitudinal integration only if β_r and $x\to 0$ together. The larger variable of x and β_r sets the scale in the small-x region. This means that $\max(x,\beta_r)$ gives the lower bound for the longitudinal integrations. Only in the small-x region, where the β components also have a strong ordering, we can get logarithms from longitudinal integrations.

According to b) and c), if we do the longitudinal and transverse integrations for the i^{th} gluon cell, the leading contribution is given by:

$$\int d\beta_i d^2p_{i\perp}\{i^{\text{th}}\text{ gluon cell}\}=g_s^2\ln\left(\frac{|p_{i+1\perp}|^2}{\max(|r_\perp|^2,\mu^2)}\right)\ln\left(\frac{\beta_{i-1}}{\max(x,\beta_r)}\right). \tag{2.3}$$

In the above expression g_s corresponds to a fixed strong coupling constant. As usual, if we take the running coupling constant, the transverse

$$\ln\left(\frac{|p_{i+1\perp}|^2}{\max(|r_\perp|^2,\mu^2)}\right)$$

is replaced by

$$\ln\ln\left(\frac{|p_{i+1\perp}|^2}{\max(|r_\perp|^2,\mu^2)}\right).$$

These are the crucial characteristics for our non-forward gluon ladders. The single gluon ladder approximation for the singlet deep inelastic structure function in the small-x region is not sufficient because it violates the Froissart bound. In this approximation the structure function behaves like $\exp\left\{\sqrt{a\ln\frac{1}{x}}\right\}$. In order to obtain a valid description of the small-x region of deep inelastic scattering we, therefore, have to take into account other diagrams.

The motivation for the choice of these diagrams comes from the Regge limit. There it is known that diagrams with only two gluon lines in the t-channel violate the unitarity bound. In order to cure this situation, diagrams with more gluon lines in the t-

channel have to be considered. Because of the intimate connection of the hard regime for small-x and the Regge limit [1], we expect that the diagrams with more gluon lines in the t-channel will improve also the behaviour of the structure function in the small-x region.

These gluon lines can interact, in principle, in all possible ways according to our kernel (Fig. 1). Obviously, any two gluon subsystem forms a non-forward ladder. We assume that for every interaction between two gluon lines the longitudinal integration has already been done and gives a $\ln\frac{1}{x}$.

The question is the following: in the hard regime, which configuration of the Feynman diagrams shown in Fig. 1, gives us the maximum number of transverse logarithms and hence the maximum enhancement for the amplitude?

We will now answer this question, first for the case of a four gluon system. In order to simplify we only consider a fixed strong coupling constant. We know that if we decompose the four gluon lines into two independent ladders, we get a certain number of transverse logarithms. The point now is to study the effect of introducing an interaction between these two ladders. We therefore shall compare the situation in Figs. 5 and 6.

There the loops 1) and 2) belong to the previous independent non-forward ladders I and II, respectively. These ladders are indicated by the arrows. In Fig. 5 we add a new loop to the first ladder, and in Fig. 6 we consider an interaction between the two ladders.

The first case of Fig. 5, according to what we said previously, gives for the transverse integrals:

$$\text{Fig. 6:}\quad \approx g_s^6 \ln^2\left(\frac{|K_{1\perp}|^2}{|r_\perp|^2}\right)\ln\left(\frac{|k_{2\perp}|^2}{|r_\perp|^2}\right). \tag{2.4}$$

Here we have not considered the other logarithms from the previous ladders. The logarithms in the above formula come, as usual, from the following phase space:

$$|r_\perp|^2 \ll |k'_{1\perp}|^2 \ll |k_{1\perp}|^2 \ll |K_{1\perp}|^2 \tag{2.5a}$$

$$|r_\perp|^2 \ll |k'_{2\perp}|^2 \ll |k_{2\perp}|^2. \tag{2.5b}$$

Now we consider Fig. 6. If the interaction between the two ladders is to be important for the leading behaviour, we want a) that the new loop does not destroy previous logarithms and b) that it provides a new hard logarithm.

As in the previous case, loops 1) and 2) give:

$$g_s^4 \ln\left(\frac{|k_{1\perp}|^2}{|r_\perp|^2}\right)\ln\left(\frac{|k_{2\perp}|^2}{|r_\perp|^2}\right). \tag{2.6}$$

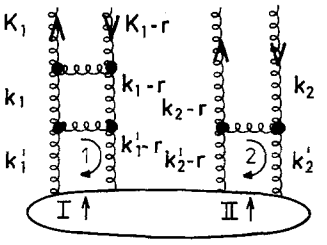

Fig. 5. A system of two independent non-forward ladders where we have added a new cell to the first ladder

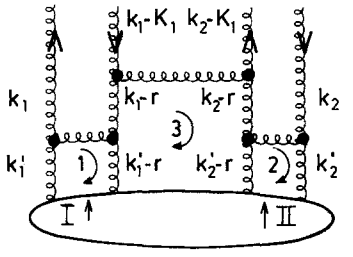

Fig. 6. An interaction between the two non-forward ladders of Fig. 5

These logarithms come from the phase space given in (2.5a) up to $|k_{1\perp}|^2$ and (2.5b). The momenta $k_{1\perp}$ and $k_{2\perp}$ are independent variables. We can have the case where $|k_{1\perp}|^2 \approx |k_{2\perp}|^2$ or, for example, $|k_{1\perp}|^2 \ll |k_{2\perp}|^2$.

For the loop 3) we have:

$$\int d^2\mathbf{r}_\perp \left\{\frac{1}{|(k_1-r)_\perp|^2}+\frac{1}{|(k_2-r)_\perp|^2} - \frac{|(k_1-k_2)_\perp|^2}{|(k_1-r)_\perp|^2|(k_2-r)_\perp|^2}\right\} \cdot \ln\left(\frac{|k_{1\perp}|^2}{|r_\perp|^2}\right)\ln\left(\frac{|k_{2\perp}|^2}{|r_\perp|^2}\right). \tag{2.7}$$

We first assume that $|k_{1\perp}|^2 \approx |k_{2\perp}|^2$. The term inside the bracket in the above formula gives a logarithm only if

$$|k_{1\perp}|^2 \approx |k_{2\perp}|^2 \ll |r_\perp|^2 \ll |K_{1\perp}|^2. \tag{2.8}$$

This condition, however, violates the initial phase space conditions given in (2.5), which are necessary in order to get not only the logarithms from the loops 1) and 2), but also all the previous enhancement from the two independent ladders. In the optimal case we would get only one logarithm of the type $\ln\left(\frac{|K_{1\perp}|^2}{|k_{1\perp}|^2}\right)$.

For all other possibilities for the phase space we also destroy the possible enhancement of the amplitude.

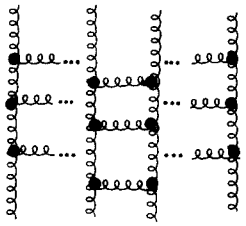

Fig. 7. A non-planar configuration of two ladders

By comparing this interacting case with the previous non interacting one (2.4) we conclude that the case without interactions between the ladders gives the maximum possible enhancement. Of course, for the interacting case any other possible rung, between the two ladders leads to the same conclusion.

From this considerations we conclude that, for the four gluon system in the hard regime, the maximum transverse enhancement is given by a configuration of two independent non-forward ladders where the momentum $r_\perp$ has to be small. This was also the choice of GLR. From our analysis we find that not only planar diagrams can be relevant. In fact the non-planar diagram also gives the maximum transverse enhancement. In Sect. IV we will give a space time argument that even favours the non-planar situation over the planar one. Actually the definition of "planar" or "non-planar" depends on the coupling of the ladders to the external lines. This will be discussed also in Sect. IV (Fig. 7).

We will now study the situation where we have an odd number of gluon lines. For this it is sufficient to consider the case of three gluon lines in Fig. 8. In this figure the arrow indicates the existence of a non-forward ladder between the first two lines. As we know, loop 1) gives us a hard transverse logarithm in the usual phase space. If we now add the second loop, which connects the ladder with the other gluon line, we can repeat our previous argument that we used for the four gluon system: we compare with the case where the second loop is added to the first ladder, and we arrive at the same conclusion as before. If we want to get a new hard transverse logarithm from the "connecting" loop 2), we have to pay the price of destroying the previous enhancement.

We could then think that, for the three gluon case, the leading behaviour will be given by a non-forward ladder and a gluon line, such that there is no interaction between them. However, such a configuration cannot survive. If we couple the three lines at the upper end of the diagram to a quark loop with high virtuality, we will have to integrate over $|r_\perp|^2$. We know that $|r_\perp|^2$ has to be small in order to provide a transverse enhancement for the ladder. In principle we can restrict the integration over $r_\perp^2$ such that the upper bound will be small. This condition will ensure that the logarithms from the ladder are large. However, this restriction of $|r_\perp|^2$ cannot be justified in perturbative QCD where the momentum k that labels a gluon propagator $G^{\mu\nu}(k)$ has to be large. In our case we will have a $G^{\mu\nu}(r)$. This means that we have to integrate $|r_\perp|^2$ up to the large external momentum, thus destroying the logarithmic enhancement from the ladder. Therefore, in the hard regime such a three gluon system is unimportant. Our conclusion for the three gluon system can be generalized to any configuration with an odd number of gluon lines. Such a configuration cannot be possible in the hard regime.

Finally we want to study the situation for a system with n gluons in the t-channel, where n is an even number $\geqq 6$. In order to do this we need to generalise our analysis of the four gluon system that we have done for the forward direction. We once again take the four gluon system, but now we permit the existence of a new momentum v that flows through the amplitude (Fig. 9). This configuration is not in the forward direction. The diagram in Fig. 9 will give two hard transverse logarithms for the loops 1) and 2) if

$$|v_\perp|^2 \approx |r_\perp|^2 \ll |k'_{1\perp}|^2 \ll |k_{1\perp}|^2$$
$$|r_\perp|^2 \ll |k'_{2\perp}|^2 \ll |k_{2\perp}|^2. \tag{2.9}$$

Our analysis for the loop 3) is not altered by the existence of the momentum v. In any case the in-

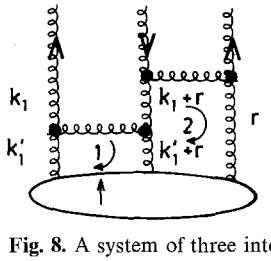

Fig. 8. A system of three interacting gluons in the t-channel

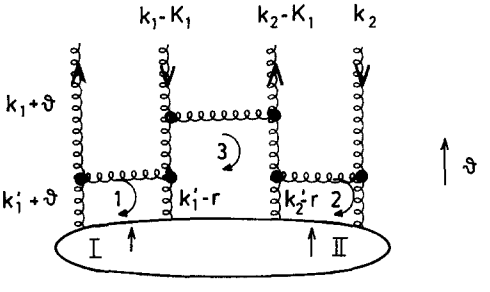

Fig. 9. A non-forward system of four interacting gluons in the t-channel

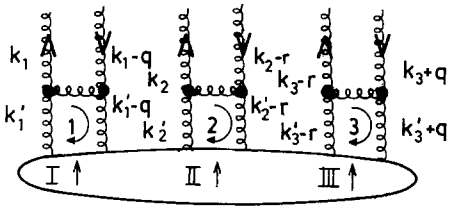

Fig. 10. A possible parametrization for the momenta of a system of six gluon lines organized into three independent non-forward ladders

tegration variable will be $r_\perp$, and then we can use our argument for the four gluon system in the forward case.

We consider now a configuration of six gluon lines. In this case we have a freedom how to parametrize the momentum of the gluon lines. There are five independent momenta and the total system must be in the forward direction. We cannot a priori favour any one of the parametrizations. In Fig. 10 we show an example, where the arrows indicate the existence of three independent gluon ladders. This means that the maximal enhancement for this system comes from the phase space where

$$|q_\perp|^2 \approx |r_\perp|^2 \ll |k'_{i\perp}|^2 \ll |k_{i\perp}|^2, \quad i=1,2,3 \tag{2.10}$$

If we introduce a connection between two ladders it is always possible to choose a parametrization for the momenta such that the four gluon system given by the two interacting ladders corresponds to the non-forward four gluon system we discussed previously (see Fig. 9). The connecting loop destroys the enhancement of the amplitude.

We can repeat this analysis for every other possible rung between two ladders with the same answer. Such kind of reasoning can be extended to 8, 10, ... etc. gluon lines.

These considerations enable us to give an answer to our initial question: For a system of n gluon lines in the t-channel (n even) which, in principle, can interact in pairs in all possible ways, the maximum transverse enhancement in the hard regime is given by a configuration of $n/2$ independent non-forward gluon ladders, and these ladders are not necessarilly in a planar configuration. If n is an odd number, all possible configurations can be neglected.

So far we have considered a system of n gluon lines organized into inpendent ladders. As we will discuss in Sect. IV, these diagrams will, in fact, be increasingly important in the small-x region. For this process we then have the following intuitive picture shown in Fig. 11. A highly virtual photon coming from the electron interacts with a quark in

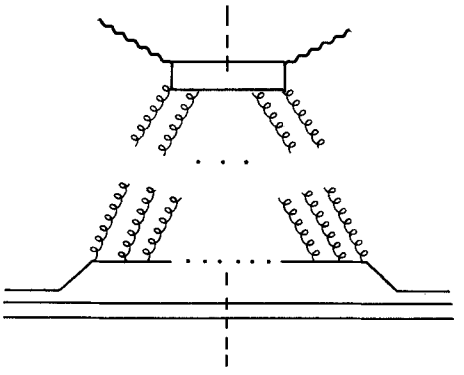

Fig. 11. The contribution of the gluon sea to the structure function in deep-inelastic scattering

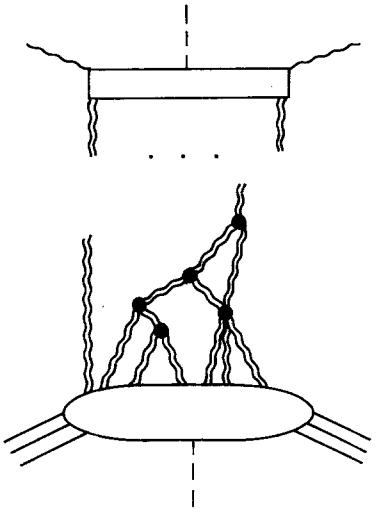

Fig. 12. A particular possible contribution to Fig. 11. The wavy lines represent gluon ladders, and the points are possible vertices where a certain number of ladders come together producing a smaller number of outgoing ladders

the gluon sea inside the photon. The sea is produced by the initial valence quarks. The scattering process finishs with the production of any possible number of hadrons, and therefore we have to take the discontinuity of the amplitude, as shown in Fig. 11.

According to our analysis the gluon sea, when looked at in the t-channel, organizes itself into independent ladders. At the upper end of the diagram these ladders must couple to a quark loop. It is also possible that two or more ladders come together producing a smaller number of ladders which also can interact again with other ladders or directly with the quark at the upper end of the diagram. A particular contribution to Fig. 11 is shown in Fig. 12 where the wavy lines represent gluon ladders and the points indicate that two or more ladders

come together producing a smaller number of ladders. A technical point in this picture corresponds to the fact that we have to integrate over the momenta that flow through the non-forward ladders. If we want to retain the maximum enhancement we have to keep all these momenta small. Finally, we have to take the discontinuity of our diagram (Fig. 11): this will be discussed in Sect. IV where we also will discuss in more detail the possible couplings between the ladders (Fig. 12).

Note that in our picture the number of ladders in the t-channel never increases if we go from the valence quarks at the bottom to the external photon at the top. This point will be also be discussed in Sect. IV.

III. Connection with the Regge Limit

In this section we want to analyse our problem from a different point of view. We start from the Regge limit and then take the limit of large transverse momentum. The idea is to see how we arrive at the hard regime of Sect. II by starting from the effective Pomeron kernel [3]. This will give us further insight into our results of the previous section. This is the analog what Dokshitzer [1] has done for the one single ladder.

In the Regge regime one starts with a small but fixed coupling constant. We have also Regge trajectories for the gluons. These trajectories are not present in Bjorken's hard regime because the diagrams that contribute to the reggeization of the gluon in the Regge regime belong, in the hard regime, to that class of Feynman diagrams which gives the running coupling constant.

The diagrams which are relevant in the Regge limit are shown in Fig. 1 where now the wavy lines represent reggeized gluons, and we have to take all possible pair interactions, mediated by the Pomeron kernel which we want to describe in a few lines. The bubbles in Fig. 1 represent here, in a first approximation, a sum over possible configurations of gluon system with $\leqq n$ gluon states. These diagrams, strictly speaking, are valid only in the neighbourhood of multiregge cut singularities; that is where reggeon unitarity and direct s-channel unitarity can be shown to be satisfied. For details see [8, 12]. In particular, the diagrams of Fig. 1 must be restricted, in the Regge regime, to the region of phase space where all $K_{i\perp}^2 \geqq \Lambda^2$ (Λ is the QCD parameter), and we introduce an infrared cutoff in order to avoid divergences.

The Pomeron kernel which includes the trajectories [3, 13, 14] is given by:

$$K_{ij}(\mathbf{k}_{i\perp}, \mathbf{k}'_{i\perp}, \mathbf{k}_{j\perp}, \mathbf{k}'_{j\perp}) = \frac{g_s^2}{(2\pi)^3} (\text{group factor } a)$$
$$\cdot \left[-(\mathbf{k}_{i\perp} + \mathbf{k}_{j\perp})^2 + \frac{\mathbf{k}_{i\perp}^2 \mathbf{k}_{j\perp}'^2 + \mathbf{k}_{i\perp}'^2 \mathbf{k}_{j\perp}^2}{(\mathbf{k}'_{i\perp} - \mathbf{k}_{i\perp})^2} \right] \frac{1}{\mathbf{k}_{i\perp}'^2 \mathbf{k}_{j\perp}'^2}$$
$$+ (\text{group factor } b)(\alpha(\mathbf{k}_{i\perp}^2) + \alpha(\mathbf{k}_{j\perp}^2)), \tag{3.1}$$

where

$$\alpha(\mathbf{k}_{i\perp}^2) = \frac{-g_s^2}{2\pi^3} \mathbf{k}_{i\perp}^2 \int \frac{d^2\mathbf{q}_\perp}{\mathbf{q}_\perp^2 (\mathbf{q}_\perp + \mathbf{k}_{i\perp})^2} \tag{3.2}$$

are the Regge trajectories. The necessity for having two group factors is discussed in [13].

If we use the Pomeron kernel *without* trajectories and take the phase space conditions (2.5a) and (2.5b) then it reduces exactly to our kernel in the hard regime. This means, of course, that we get the same conclusions as before. Only independent ladders are dominant in the hard regime.

Apart from the configuration of two separate ladders where the transverse logarithmic factors arises in the standard way, there is now still another source of logarithmic enhancement factors. In constrast to the "hard logs" these factors, however, are sensitive to the infrared region and, hence, not purely perturbative.

In a recent paper [15] Jaroszewicz and Kwieciński tried to solve the integral equation for a system of three gluon lines in the Regge limit. In their analysis they considered the possible sources for large transverse logarithms. They found two sources: a) the usual phase space conditions for the enhancement of a non-forward ladder, and b) larger ratios of virtualities of the interacting gluon lines. If the three momenta are scaled uniformely the integral equation does not lead to logarithms.

We now want to do the same analysis for the forward four gluon system, using the full Pomeron kernel *with* trajectories. In particular we will analyse the interacting case of Fig. 6 where we take large differences between the virtualities of the interacting gluons.

For the loop 3) of Fig. 6 we than have:

$$\int d^2\mathbf{r}_\perp \left\{ \left[\frac{-(\mathbf{k}_{1\perp} - \mathbf{k}_{2\perp})}{(\mathbf{k}_1 - \mathbf{r}_\perp)^2 (\mathbf{k}_2 - \mathbf{r}_\perp)^2} + \frac{(\mathbf{k}_{1\perp} - \mathbf{K}_{1\perp})^2}{(\mathbf{K}_{1\perp} - \mathbf{r}_\perp)^2 (\mathbf{k}_1 - \mathbf{r}_\perp)^2} \right.\right.$$
$$\left. + \frac{(\mathbf{k}_2 - \mathbf{K}_{1\perp})^2}{(\mathbf{K}_{1\perp} - \mathbf{r}_\perp)^2 (\mathbf{k}_{2\perp} - \mathbf{r}_\perp)^2} \right] \cdot (\text{group factor } a)$$
$$- \left[\frac{(\mathbf{k}_{1\perp} - \mathbf{K}_{1\perp})^2}{\mathbf{r}_\perp^2 (\mathbf{k}_{1\perp} - \mathbf{K}_{1\perp} + \mathbf{r}_\perp)^2} + \frac{(\mathbf{k}_2 - \mathbf{K}_{1\perp})^2}{\mathbf{r}_\perp^2 (\mathbf{k}_{2\perp} - \mathbf{K}_{1\perp} + \mathbf{r}_\perp)^2} \right]$$
$$\left. \cdot (\text{group factor } b) \right\} \cdot \ln \left(\frac{\mathbf{k}_{1\perp}^2}{\mathbf{r}_\perp^2} \right) \ln \left(\frac{\mathbf{k}_{2\perp}^2}{\mathbf{r}_\perp^2} \right). \tag{3.3}$$

Here the two logarithms come from the first two loops in Fig. 6 and the second square bracket represents the trajectory functions of (3.1). As we said before, we take different virtualities. We choose

$$\mathbf{k}_{1\perp}^2 \approx (\mathbf{k}_{1\perp}-\mathbf{r}_\perp)^2 \ll \mathbf{k}_{2\perp}^2 \approx (\mathbf{k}_{2\perp}-\mathbf{r}_\perp)^2 \tag{3.4}$$

for the momenta before the interaction between the two ladders.

The point now is to get new logarithms without destroying the previous enhancement. If we insist on having the same relative kinematical configuration (3.4) also after the interacting loop 3), i.e.

$$\mathbf{k}_{1\perp}^2 \approx (\mathbf{k}_{1\perp}-\mathbf{K}_{1\perp})^2 \ll \mathbf{k}_{2\perp}^2 \approx (\mathbf{k}_{2\perp}-\mathbf{K}_{1\perp})^2 \tag{3.5}$$

this means that $\mathbf{r}_\perp^2 \approx \mathbf{K}_{1\perp}^2$ and we will not get a justifiable logarithm from the term inside the bracket in formula (3.3). By justifiable we mean that in this case we have a gluon propagator $G^{\mu\nu}((\mathbf{K}_{1\perp}-\mathbf{r}_\perp)^2)$ where the virtuality $(\mathbf{K}_{1\perp}-\mathbf{r}_\perp)^2$ is very small. We feel here the infrared unstability and the necessity for an infrared cutoff.

In order to get a logarithm it is necessary to allow other kinematical configuration after the interacting loop. For example, we try

$$\mathbf{k}_{2\perp}^2 \gg \mathbf{K}_{1\perp}^2 \gg \mathbf{k}_{1\perp}^2. \tag{3.6}$$

If we take an integration interval for $\mathbf{r}_\perp^2$ such that

$$\mu^2 \ll \mathbf{r}_\perp^2 \ll \mathbf{k}_{1\perp}^2 \left(\frac{\mathbf{k}_{1\perp}^2}{\mathbf{K}_{1\perp}^2}\right), \tag{3.7}$$

then the leading contribution for the $\mathbf{r}_\perp$ integral in (3.3) is given by

$$\int d^2\mathbf{r}_\perp \{\ldots\} \approx (\text{group factor } b) \ln^3 \left(\frac{\mathbf{k}_{2\perp}^2}{\mathbf{k}_{1\perp}^2}\right). \tag{3.8}$$

Owing to the phase space condition (3.6), we see that the integral gives us a new hard logarithm without destroying the contribution of the previous two logarithms. This new logarithm, however, comes from the trajectories. It is clear that if we scale the momenta of the four gluon lines uniformely we do not have this type of effect. In the case of three gluons [15] it was not necessary to take different kinematical configurations but for our case this conditions turns out to be essential in order to get this new type of hard transverse logarithm. If we take new loops into account it would be possible to collect such type of logarithms by using a complicated set of coupled kinematical configurations.

In the hard regime, as we said, there are no trajectories but a running coupling constant and we will not have these logarithms. However, if we go to extreme small values, such that our analysis and also that of GLR is no longer valid, it is not clear what happens with the running coupling constant. It could be that the trajectories become important, and, therefore, the above logarithms cannot be ignored. We would have then a connection between Bjorken's hard regime and the Regge limit. In any case we know from unitarity that there will be non perturbative effects [8] which build the Pomeron and hadronic total cross sections.

The conclusions for this section are the following:

a) If we analyse the system of gluon states that we studied in the previous section, using now the Pomeron kernel without trajectories in the limit of high transverse momentum, we get an agreement with our results of Sect. II. The leading behaviour is given by a set of independent non-forward gluon ladders.

b) If we include the trajectories, there are some regions of phase space where these trajectories yield transverse logarithms for the interaction between two ladders if the interacting gluons have vastly different virtualities. However, these logarithms are not entirely "hard" but sensitive to the infrared region, and one needs the existence of an infrared cutoff.

IV. Non-planar Couplings Between Ladders

We now have to analyse in somewhat more detail how the gluon configurations of Sect. II contribute to the small-x behaviour of the structure function of deep inelastic scattering. Our main result of Sect. II was that, among diagrams with n gluon lines (n even) only configurations with independent non-forward ladders dominate. These ladders are able to come together producing a smaller number of ladders or, in a particular case, a single ladder. Alternatively, a single ladder can split into two non-forward ladders. In this section we want to discuss such couplings.

The simplest situation corresponds to the case where two ladders come together producing a single ladder. We have different possibilities for such a coupling:

a) The first case is the planar coupling shown in Fig. 13. This was the configuration taken by GLR in their analysis.

b) The second possibility corresponds to the maximal non-planar case shown in Figs. 14a, b. In Regge physics this case is the so called Mandelstam crossing.

c) The third case is given by a mixed configuration between the planar and the maximal non-planar situation as shown in Figs. 15a, b.

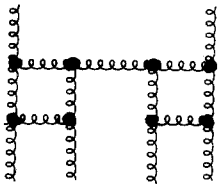

Fig. 13. The planar vertex where two ladders go into a single ladder

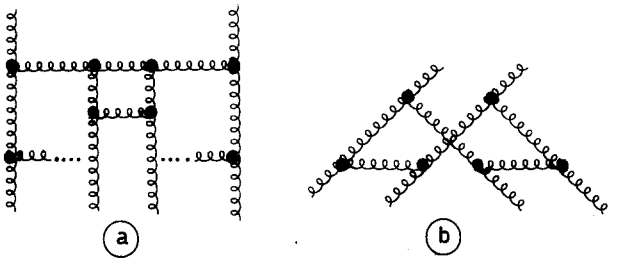

Fig. 14. a The maximal non-planar vertex for two ladders with a single outgoung ladder. **b** A different perspective of the maximal non-planar vertex in a

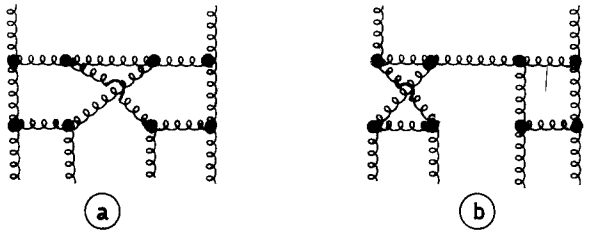

Fig. 15. a A mixed vertex for two ladders with a single outgoing ladder. **b** Another example of a mixed case where one of the incoming ladders in Fig. 13 has been twisted

Figure 15b represents a planar coupling between two ladders where one of them is twisted. Of course the diagram is a non-planar one.

So far we have considered the full amplitude with n independent gluon ladders. If we want to decompose this amplitude into its possible discontinuities we need to know how the different cuts contribute. This question has been an old problem in Regge physics, and the answer is given by the so called AGK rules (Abramovskii, Gribov, Kancheli) [5]. We will see that in our case the AGK rules are in fact valid.

First we want to study the maximal non-planar coupling (Fig. 16). In this figure we have taken the double multiperipherical cut. In our analysis we will assume a running coupling constant. For the phase space conditions we choose first

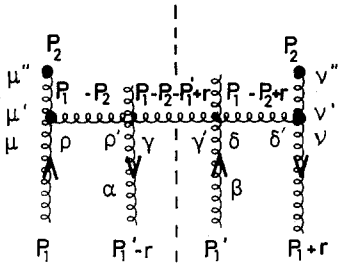

Fig. 16. The maximal non-planar vertex where two ladders go into one single ladder with the double multiperipherical cut

$$\beta_{P_1} \approx \beta'_{P_1'} \approx \beta_r \gg \beta_{P_2}$$
$$|P_{2\perp}|^2 \gg |P_{1\perp}|^2 \approx |P_1'|^2 \gg |r_\perp^2|. \tag{4.1}$$

This condition defines the hard regime where the two ladders are significant in the small-x region.

The non-planar coupling without color factors, which give only a group coefficient, is given by:

$$\begin{aligned}
&\int \frac{d^4P_2}{(2\pi)^4} 16\pi^2 \alpha_s^2(|P_{2\perp}|^2)\, 2\pi\delta_+((P_1-P_2-P_1'+r)^2)\\
&\cdot (P_1-P_2)^{-2}(P_1-P_2+r)^{-2}P_2^{-4}\\
&\cdot \{d_{\mu''\mu'}(P_2)\Gamma_{\mu\mu'\rho}(P_1,P_2,P_1-P_2)d_{\rho\rho'}(P_1-P_2)\\
&\cdot \Gamma_{\alpha\rho'\gamma}(P_1'-r,P_1-P_2,P_1-P_2-P_1'+r)d_{\gamma\gamma'}(P_1-P_2-P_1'+r)\\
&\cdot \Gamma_{\beta\gamma'\delta}(P_1-P_2-P_1'+r,P_1',P_1-P_2+r)d_{\delta\delta'}(P_1-P_2+r)\\
&\cdot \Gamma_{\gamma\delta'\nu'}(P_1-r,P_1-P_2-r,P_2)d_{\nu'\nu''}(P_2)\delta_{\mu\nu}\delta_{\alpha\beta}\}.
\end{aligned} \tag{4.2}$$

In this formula $\Gamma_{\alpha\beta\gamma}(P_1,P_2,P_3)$ denotes the well known three gluon vertex coupling and $d_{\alpha\beta}(k)$ corresponds to the numerator of the gluon propagator $G_{\alpha\beta}(k)$ which is given by:

$$G_{\alpha\beta}(k)=\frac{d_{\alpha\beta}(k)}{k^2+i\varepsilon}. \tag{4.3}$$

In the axial gauge we have

$$d_{\alpha\beta}=g_{\alpha\beta}-\frac{k_\alpha c_\beta + c_\alpha k_\beta}{(k\cdot c)}. \tag{4.4}$$

For the gauge fixing vector c_α we choose, following [7], the Sudakov momentum q'_α. This is very convenient because we can read directly the β dependence of the coupling. We have $c^2=0$ which simplifies the calculations.

From the δ function in (4.2), using the phase space conditions (4.1) we get the α component of P_2

$$\alpha_{P_2}=\frac{-|P_{2\perp}|^2}{2(\beta_{P_1}-\beta'_{P_1'}+\beta_r)v}. \tag{4.5}$$

The important terms which dominate in the small-x case will be proportional to

$$\frac{P_{2\mu''}P_{2\nu''}|P_{2\perp}|^2}{\beta_{P_2}^2}. \tag{4.6}$$

If we use the phase space (4.1) we obtained a very long and complicated expression for the coefficient of (4.6) which is not interesting. It is possible to simplify enormeously our calculation if we regard the non-planar coupling from a different perspective, as shown in Fig. 17. In this figure we see that actually the gluons with momentum P_1-P_2 and P_1-P_2+r are the last gluons of the non-forward ladder indicated by the arrow. Therefore, in order to have the maximum longitudinal enhancement for this ladder we need to take the new phase space conditions

$$\begin{aligned}&\beta'_{P_1'} \gg \beta_{P_1} \approx \beta_r \gg \beta_{P_2}\\ &|P_{2\perp}|^2 \gg |P_{1\perp}|^2 \approx |P'_{1\perp}|^2 \gg |r_\perp|^2,\end{aligned} \tag{4.7}$$

which replace condition (4.1).

The phase space conditions (4.7) simplify our initially complicated expression. For the term inside the bracket in (4.2) we get

$$\{\}_{(4.2)} \approx \frac{|P_{2\perp}|^2 P_{2\mu''}P_{2\nu''}}{\beta_{P_2^2}}\beta_{P_1}\beta'_{P_1'}. \tag{4.8}$$

This expression coincides with the result for the planar case.

Actually, as we will show in a few lines by studying the full diagram, the relevant phase space conditions for the coupling of the two ladders will be given by

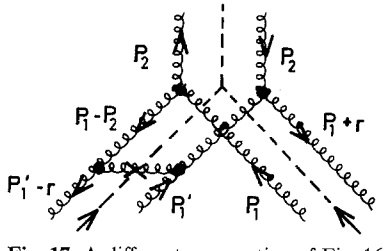

Fig. 17. A different perspective of Fig. 16

$$\begin{aligned}&\beta'_{P_1'} \gg \beta_{P_1} \gg \beta_{P_2} \gtrsim \beta_r\\ &|P_{2\perp}|^2 \gg |P_{1\perp}|^2 \approx |P'_{1\perp}|^2 \gg |r_\perp|^2.\end{aligned} \tag{4.9}$$

Other cuts of the diagram give the same answer for the vertex. If we take the multiperipherical cut shown in Fig. 18a (in this figure we have also shown a rung of the second ladder which is denoted by the arrow), we do not have a δ-function for the α_{P_2} integral but three propagators. By using the $+i\varepsilon$ precription for the propagators we see that the propagator with momentum $P_1-P_2-P_1'+r$ has a pole in the lower complex half plane α_{P_2} because $\beta'_{P_1'} \gg \beta_{P_1}\beta_r$. The other two propagators have a pole in the upper half plane. We close then our α_{P_2}-contour in the lower half plane, getting the same answer as for the double multiperipherical cut.

If we take now the diffractive cut, Fig. 18b, the $\delta((P_1-P_2+r)^2)$ implies

$$\alpha_{P_2} = \frac{-|P_{2\perp}|^2}{(\beta_{P_1}+\beta_r)v} \approx \frac{-|P_{2\perp}|^2}{\beta_{P_1}v}, \tag{4.10}$$

where we have used (4.7).

The AGK rules are, in fact, valid, because the result for the vertex, in the relevant phase space (4.9), does not depend on which cut we take.

We have also studied the mixed cases (Figs. 15a, b). We again get an answer of the form (4.8) if we demand the phase space condition (4.9).

At this point we can discuss other possibilities where, for example, three ladders come together in the maximal non-planar configuration producing a single ladder (Fig. 19), or the case where three ladders combine into a final configuration of two ladders (Fig. 20).

In both cases we have more powers of the running coupling constant than in the previous situation. They depend on transverse momenta with the largest virtuality at each vertex. There are also more propagators depending on these highly virtual momenta. The crucial point, however, is that we do not have here new loops with could give a transverse enhancement in order to compensate the effect of the running coupling constants and of the propagators. We conclude that the contribution of such

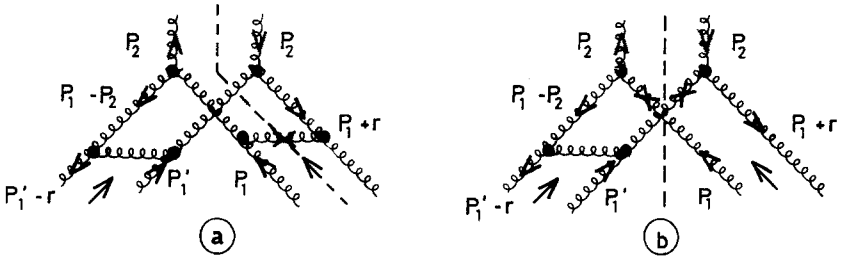

Fig. 18. a One of the multiperipherical cuts of the diagram in Fig. 17. We have added a rung which belongs to the second ladder. **b** The diffractive cut of the diagram in Fig. 17

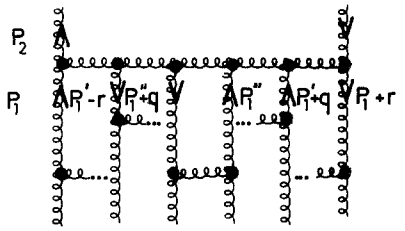

Fig. 19. The maximal non-planar vertex where three ladders come together producing a single outgoing ladder

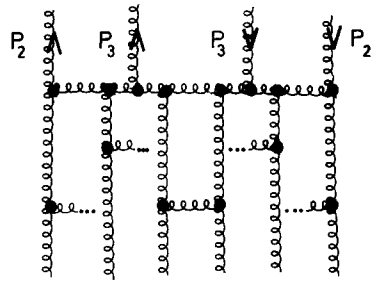

Fig. 20. Three ladders in a maximal non-planar configuration come together producing two outgoing ladders

couplings will be small. If three ladders have to combine, it is, therefore, more profitable that this occurs in steps: first two ladders combine producing a single ladder, then this ladder combines with the other one.

We can generalize this argument to more complicated diagrams where 4, 5... etc. gluon ladders come together producing a smaller number of ladders. The most convenient way to do this is to organize the process in steps where, at each step, two ladders combine producing a single ladder which, in the next step, comes together with another ladder, and so on.

In order to complete our analysis of the maximal non-planar configuration we want to study the lower vertex where a forward ladder branches into two non-forward ladders (further up in the diagram, these ladders come together again according to the coupling we discussed above). The branching vertex is shown in Fig. 21, and the full diagram in Fig. 22. We are doing this in order to estimate the relevance of diagrams á la Fig. 22: is it possible that, when going from the valence quarks at the bottom to the photon at the top of the diagram, we start with two gluon lines, then the number of gluons increases, and, eventually diminishes again? In agreement with GLR, we will see that such a diagram is not important. The leading contribution will always be given by a diagram where the number of gluon lines never increases.

Now we will discuss the lower branching vertex

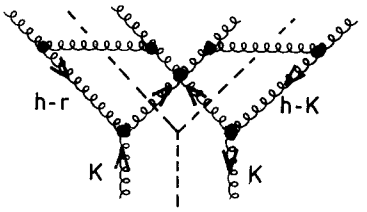

Fig. 21. The non-planar branching vertex where a ladder goes into two non-forward ladders

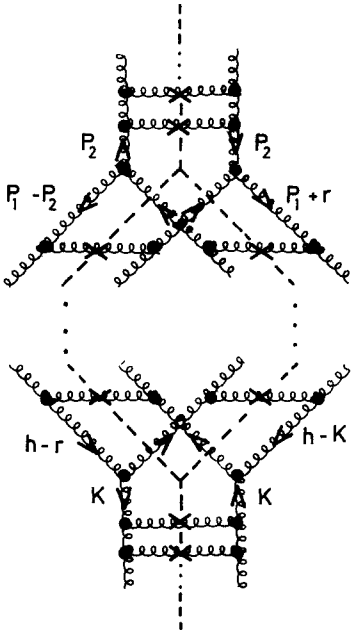

Fig. 22. A maximal non-planar multiladder diagram with the double multiperipherical cut

shown in Fig. 21. Here we have taken the double multiperipherical cut. After calculations along the lines of [4] we find for the numerator of the lower vertex.

$$\text{Numerator}_{\text{Lower vertex}} = \frac{8Ng_s^2(|h_\perp|^2)\cos\alpha}{\beta(1-\beta)} \cdot \left[\beta(1-\beta)+\frac{1-\beta}{\beta}+\frac{\beta}{1-\beta}\right]|(h-r)_\perp||h_\perp|. \tag{4.11}$$

In this formula α represents the angle between $\mathbf{h}_\perp$ and $(\mathbf{h}-\mathbf{r})_\perp$, β the fraction of the longitudinal component of K carried by h (here we have taken $\beta_K=1$) and $g_s^2(|h_\perp|^2)$ is the running coupling constant. During the calculation we have neglected β_r because $\beta_r \ll \beta_h$ if the ladders have to give a non vanishing contribution, and we have taken the hard regime condition $|h_\perp|^2 \gg |K_\perp|^2$.

In formula (4.11) we recognise the Altarelli-Parisi [16] kernel for the three gluon system and, if we

consider $\beta \ll 1$ (i.e. the small-x case), we recover essentially our old expression for one rung in the non-forward ladder [4].

Now we can study the full maximal non-planar diagram shown in Fig. 22. We assume the existence of the running coupling constant, as a result of which the transverse $\ln\left(\frac{K_\perp^2}{r_\perp^2}\right)$ turns into $\ln\ln\left(\frac{K_\perp^2}{r_\perp^2}\right)$, and we introduce our old variable

$$\xi_k = \int_{\max(\mu^2,|r_\perp|^2)}^{|k_\perp^2|} \frac{\alpha_s(|k'_\perp|^2)}{|k'_\perp|^2} \frac{d|k'_\perp|^2}{4\pi}.$$

By y_k we want to denote $\ln\frac{1}{\beta_k}$. We further remember that a non-forward gluon ladder with external variables β_K and $|K_\perp|^2$ where $|K_\perp|^2 \gg |r_\perp|^2$ and $\beta_K > \beta_r$ behaves like

$$D(\xi_K, y_K) \underset{y_K \text{ large}}{\approx} e^{\sqrt{16N\xi_K y_K}}, \quad N=3. \tag{4.12}$$

If we glue to Fig. 17a ladder beginning at P_2 which goes up to the external photon and a lower non-forward ladder to the lines with momentum P_1 and P_1+r, we get a factor β_{P_2} from the next rung in the upper ladder and a factor

$$\frac{1}{\beta_{P_1}(\beta_{P_1}+\beta_r)} \cdot \frac{\alpha_s(|P_{1\perp}|^2)}{|P_{1\perp}|^2}, \quad (|P_{1\perp}|^2 \gg |r_\perp|^2)$$

from the fact that we have now a cell in a non-forward ladder.

We must combine this with (4.8) where we introduce a $\delta_{\mu''\nu''}$. For this coupling, appart from numerical factors, we have then

$$\frac{\alpha_s^2(|P_{2\perp}|^2)\alpha_s(|P_{1\perp}|^2)}{\beta_{P_2}(\beta_{P_1}+\beta_r)|P_{1\perp}|^2|P_{2\perp}|^4}. \tag{4.13}$$

The factor $\beta'_{P'_1}$ in (4.8) has been combined with the factor $\frac{1}{\beta'^2_{P'_1}}$ coming from the corresponding cell in the non-forward ladder ($\beta'_{P'_1} \gg \beta_r$) producing the desired longitudinal logarithm.

After this preliminaries we can write a formula for the multiladder diagram shown in Fig. 22: (y_q and ξ_q refer to the photon external variables)

$$\begin{aligned}
\text{Fig. 22: } & \alpha \int dy_{P_2} d\xi_{P_2} \int d\beta_r d^2|\mathbf{r}_\perp| \int \frac{d\beta_1}{(\beta_1+\beta_r)} d\xi_{P_1} \\
& \cdot \int d\beta_h d^2\mathbf{h}_\perp D(y_q - y_{P_2}, \xi_q - \xi_{P_2}) \frac{\alpha_s(|P_{2\perp}|^2)}{|P_{2\perp}|^2} \\
& \cdot \Big\{ D(\min(y_{P_1}, y_r) - y_h;\ \xi_{P_1} - \max(\xi_h, \xi_r)) \\
& \cdot D(\min(y_{P_1}, y_r) - y_h, \xi_{P_2} - \max(\xi_h, \xi_r)) \\
& \cdot \int d\beta_K d\xi_K \frac{\beta_K^2}{\beta_h^2} \frac{\alpha_s(|h_\perp|^2)}{|(h-r)_\perp||h_\perp|} D(\xi_K, \beta_K) \Big\}.
\end{aligned} \tag{4.14}$$

Before we analyse the dominant contributions in this formula we want to make some remarks: a) In the above expression we have calculated α_h and α_r from the branching vertex and, therefore, we have left only two propagators for this vertex. b) For the branching vertex we have taken into account only the most singular contribution, assuming the strong ordering $\beta_h \ll \beta_K$ which is valid in the small-x region. c) The min's and max's in the argument of the non-forward ladders take into account what we said in Sect. II about the transverse and longitudinal enhancement of a non-forward ladder. d) The above expression assumes the phase space condition

$$\begin{aligned}
& |q_\perp|^2 \gg |P_{2\perp}|^2 \gg |P_{1\perp}|^2 \gg |h_\perp|^2 \approx |r_\perp|^2 \gg |K_\perp|^2 \\
& \beta_q = x \ll \beta_{P_2} \ll \beta_{P_1} \approx \beta_r \ll \beta_h \ll \beta_K
\end{aligned} \tag{4.15}$$

which is the natural one for the longitudinal and transverse enhancement of the ladders in the hard regime for the small-x case.

In order to get a large longitudinal enhancement from the integration in β_{P_1} we need a small β_r. We know that β_r plays the rôle of a longitudinal cutoff for the non-forward ladders. If we have a region of phase space where $\beta_{P_1} \lesssim \beta_r$ we can neglected its contribution to the integration. Only if $\beta_r \lesssim \beta_{P_2} \ll \beta_{P_1}$ we will have a significant longitudinal enhancement. This justifies the phase space conditions given by (4.9). The lower bound for the β_{P_1} integration will then be given by β_{P_2}. It is also clear that we need $\beta_h \approx 1$ in order to get a large longitudinal contribution. Concerning the ξ_{P_1} integral, the natural upper bound is given by ξ_{P_2}. The dominant contribution for the integrals will come from a region where $\beta_{P_2} \lesssim \beta_{P_1}$ and $|P_{1\perp}|^2 \lesssim |P_{2\perp}|^2$.

For the transverse enhancement it is crucial that $|h_\perp|^2$ must be very small and also $|r_\perp|^2 < |h_\perp|^2$, otherwise the non-forward ladders become irrelevant. All these conditions, combined with the necessity that $\beta_h \ll \beta_K$, $|h_\perp|^2 \gg |K_\perp|^2$, imply that there is not sufficient phase space in order to have the lower ladder $D(\xi_K, y_K)$ without destroying the possible enhancement.

The most convenient situation corresponds to the case where we do not have the lower forward ladder, and, therefore, the non-forward ladders couple directly to the valence quarks. Another argument for this conclusion is the existence of the running coupling constant at the lower vertex $\alpha_s(|k_\perp|^2)$. It is clear that the diagram shown in Fig. 22 will become more significant if $|h_\perp|^2 \approx \Lambda^2$ and the loop actually has to begin at the valence quarks. This conclusion agrees with the planar analysis of GLR and gives support to our picture at the end of Sect. II. From our discussion we see that β_r and $|r|^2$ have to be kept as small as possible.

The vertex where two ladders come together producing a single ladder behaves like $\frac{\alpha_s(|P_{2\perp}|^2)}{|P_{2\perp}|^2}$ and, therefore, such diagrams do not belong to the leading logarithmic approximation. This beviour, however, enables us to go into smaller-x values. We compensate the $\frac{\alpha_s(|P_{2\perp}|^2)}{|P_{2\perp}|^2}$ contribution by an enhancement in $\ln\frac{1}{\beta_{P_2}}$.

Like in the planar case, the leading contribution for (4.14), neglecting the lower ladder will correspond to.

$$\int dy_{P_2} d\xi_{P_2} D(y_q - y_{P_2}, \xi_q - \xi_{P_2}) \cdot \frac{\alpha_s(|P_{2\perp}|^2)}{|P_{2\perp}|^2} D^2(y_{P_2}, \xi_{P_2}) \approx \exp\left[\sqrt{16N\xi_q y_q} + \frac{3}{4}\sqrt{\frac{16N_c y_q}{b^2\xi_q}} \ln\frac{8N y_q}{b^2\xi_q}\right]. \quad (4.16)$$

The contribution of (4.16) to the structure function turns out to be more dangerous for unitarity than a single ladder. Therefore we need to sum an infinite number of diagrams. In Fig. 4 we have shown how these diagrams look like. (The wavy lines represent gluon ladders.) Apart from the non-planarity of the relevant diagrams and connected with this the sign structure of the various discontinuities, our conclusions so far basically agree with those of [7]. As a result of this, the technique of how to sum all the diagrams in the small-x limit can inmediately be taken from [7]. We, therefore, do not need to repeat this part of their analysis and only quote results. We first remark that these diagrams are important in the phase space region where

$$\frac{1}{2} e^{2b\xi_0} b\xi < \frac{8N}{b} y_q < e^{2b\xi_q}$$

$\left(\xi_q = \frac{1}{b}\ln\ln\frac{Q^2}{\Lambda^2},\ y_q = \ln\frac{1}{x}\right.$ are the external photon variables$\left.\right)$. ξ_0 in this expression corresponds to $\frac{1}{b}\ln\ln\frac{q_0^2}{\Lambda^2}$ where q_0^2 is the target mass which must be large enough ($\alpha_s(q_0^2) < 1$) so that perturbation theory remains valid. If $\frac{8N}{b} y_q > e^{2b\xi_q}$ we need other contributions, and, as we said in Sect. III, we cannot expect to analyse the limit where $x \to 0$ with these methods.

A crucial point concerning the summation of the dominant multiladder "fan" diagrams is the necessity for an alternating series in order to get convergence. This can be justified only by means of the AGK rules.

It is interesting to remark that for our branching vertex of Fig. 21 it is not true, as we said in [4], that the diffractive cut gives the same answer as the double multiperipherical cut we used here. However, for the dominant diagrams where the number of gluon ladders never increases when going from the valence quarks to the photon, the branching vertex does not play any rôle and, therefore, the analysis of GLR, where the AGK rules are needed, remains valid.

In order to complete the discussion we give now the structure function coming from the summation of the dominant planar diagrams [7]. According to our analysis there will be also diagrams which corresponds to non-planar configurations, but their contribution do not alter the qualitative behaviour of the structure function which is given by:

$$D(y_q, \xi_q) \approx \cdot \exp[\sqrt{16N(\xi_q - \tilde{\xi}(\xi_q, y_q))(y_q - \tilde{y}(\xi_q, y_q)} + e^{b\tilde{\xi}(\xi,y)}]. \quad (4.17)$$

The parameters $\tilde{\xi}(\xi, y)$ and $\tilde{y}(\xi, y)$ temper the enhancement of the structure function for small-x values. As we said, this formula is only valid for

$$e^{b\xi_0} \ln\ln\frac{Q^2}{\Lambda^2} < \frac{8N}{b}\ln\frac{1}{x} < e^{2\ln\ln\frac{Q^2}{\Lambda^2}}.$$

Before we conclude this section, we want to mention a space-time argument which shows that the vertex where two ladders combine into one ladder in a planar configuration will be less probable than the case where the two ladders are in maximal non-planar configuration.

Space-time considerations can be found in [17, 18], and also in the paper by GLR [7].

In Fig. 23 we have represented the planar situation in a time picture. In this figure the first ladder results from an excitation of the sea where an initial gluon produces other gluons which become slower

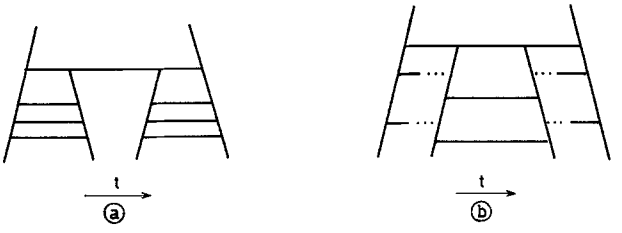

Fig. 23. a A time description for the interaction of two ladders in a planar configuration. **b** A time description for the interaction of two ladders in a maximal non-planar configuration

and slower and, at the same time, get larger virtualities. At a certain point the partons start to recombine again, first the slow gluons with large virtualities, until the fluctuation has come to an end. It is important to note that the lifetime of the partons diminishes along the ladder. The lifetime is given by $t_i=\frac{1}{\Delta E_i}$, where ΔE_i is the energy difference after and before the emission of the parton. It can be shown (for the details see [7]) that the lifetime of the i^{th} parton is given by $t_i\approx\frac{2\beta_i|\mathbf{P}|}{k_{i\perp}^2}$. Here $|\mathbf{P}|$ corresponds to the longitudinal momentum of the initial parton in the ladder.

From the high virtuality region of the fluctuation we have a remaining gluon left with high virtuality. After the first fluctuation has finished, a second fluctuation has to start until it develops virtualities comparable of the "hanging" gluon from the first fluctuation. Only then an interaction between the two fluctuations can take place. We see that this process demands a rather long time whereas the connecting parton has a small lifetime because of its large virtuality.

On the other side a maximal non-planar configuration, represented in Fig. 23b, will corresponds to two simultaneous excitations, two ladders, that can overlap in the configuration space. It is clear that the partons which mediate the interaction do not need much time, because everything occurs, more as less, at the same time.

According to these ideas we can also understand the fact that the interaction between two gluons will be more probable if they have the same $\mathbf{k}_\perp$.

V. Conclusions

In this paper we have studied, in the small-x limit of the Bjorken region, Feynman diagrams which contain more than two gluons in the t-channel. The main motivation for this comes from the well known fact that a single ladder, in the limit $x\to 0$, leads to a wrong description. Investigations of the Regge limit, on the other hand, strongly indicate that gluon configurations with a large number of gluons in the t-channel are required. This suggests that the usual one-ladder description of the Bjorken region of deep inelastic scattering, when approaching the small-x limit, has to be corrected by taking into account diagrams with more than two gluon lines in the t-channel.

We have analysed in the hard regime diagrams with an arbitrary number of gluon lines which can interact in pairs in all possible ways. For every such interaction between two gluon lines we used the non-forward kernel found in a previous paper [4]. From this analysis we have concluded that among all possible Feynman diagrams with these characteristics, only independent non-forward ladders give the maximum transverse enhancement for the amplitude. A configuration with an odd number of lines cannot survive in the hard regime. The system of independent ladders must not necessarily be a planar configuration.

By studying this gluon system in a different way, namely coming from the Regge limit we found, as expected, an agreement with the above conclusions: in the region of high transverse momentum, the Pomeron kernel (without trajectories) coincides with the small-x kernel in the hard regime. If we include the trajectories, there are some regions of phase space where these trajectories yield transverse logarithms for the interaction between two ladders, if the interacting gluons have vastly different virtualities. These logarithms, however, are sensitive to the infrared region and one feels the existence of an infrared cutoff. In any case, in the hard regime, we do not have Regge trajectories, and these new logarithms signal the on set of Regge-dynamics.

The gluon system, which organizes itself into independent ladders, gives a contribution to the singlet deep inelastic structure function. It is possible that two or more independent ladders come together producing a smaller number of outgoing ladders when going from the valence quarks to the external photon. The most elementary vertex where two ladders go into one single ladder is the most relevant case. This vertex behaves like $\frac{\alpha_s(|k_\perp|^2)}{|k_\perp|^2}$ and, therefore, does not belong to the leading logarithmic approximation. This fact, however, enables us to go to smaller-x values by compensating the small transverse factor $\frac{\alpha_s(|k_\perp|^2)}{|k_\perp|^2}$ with a large longitudinal logarithm $\ln\frac{1}{\beta_k}$. For other couplings, for example where three ladders go into one or two ladders, we do not have such a compensating factor and, therefore, they can be neglected.

We have analysed in detail the maximal non-planar coupling of two ladders and also the maximal non-planar multiladder diagram with two ladders. From our analysis we conclude that the case where an initial ladder branches into two non-forward ladders, and then these ladders recombine again into a single ladder when going from the valence quarks to the photon is not relevant. The existence of the lower ladder destroys the enhancement of the multiladder diagram. The non-forward

ladders must couple directly to the valence quarks. Therefore, in general, for an initial number of gluon lines, organized into independent ladders, the number of gluons never increases when going to the photon at the upper end of the diagram. An important point is the fact that the non-forward momentum which flow through the ladders must be kept small by hand; otherwise we destroy the enhancement of the diagram.

In the relevant phase space region the maximal non-planar vertex coincides with the planar one. For this maximal non-planar vertex we verify the validity of the AGK rules because the vertex does not depend on the cut we use. A space-time argument tells us, in fact, that the case where two ladders couple in a maximal non-planar way is more likely than the planar configuration.

These results basically confirm the analysis of GLR [7]. We disagree, however, in that our analysis favour non-planar diagrams over planar ones, whereas GLR only considered planar diagrams. Despite this disagreement, we nevertheless confirm their main conclusion, in particular, their result of summing all the diagrams: the small-x behaviour is less divergent than that of a single gluon ladder, and the perturbative description breakes down if x is smaller than a certain function of Q^2.

Finally, our analysis gives a first idea of what happens when we go to even smaller-x: certain contributions which are infrared sensitive enter into the analysis and this confirms the believe that the limit $x \to 0$ eventually requires non perturbative contributions.

Acknowledgements. I want to express my gratitude to Professor J. Bartels for his permanent support and for many discussions. I acknowledge the financial support of the Deutscher Akademischer Austauschdienst (DAAD) and of the Vicerrectoria Académica of the Universidad Católica de Chile.

References

1. Yu.L. Dokshitzer: Sov. Phys. JETP **46**, 641 (1977)
2. Yu.L. Dokshitzer, D.I. Dyakonov, S.T. Troyan: Phys. Rep. **58**, 269 (1980)
3. E.A. Kuraev, L.N. Lipatov, V.S. Fadin: Sov. Phys. JETP **45**, 199 (1977)
4. J. Bartels, M. Loewe: Z. Phys. C - Particles and Fields **12**, 263 (1982)
5. V.A. Abramovskii, V.N. Gribov, O.V. Kancheli: XVI International Conference on High Energy Physics, Chicago Batavia Vol. 1, 389 (1972)
6. L.V. Gribov, E.M. Levin, M.G. Ryskin: Phys. Lett. B**101**, 185 (1981)
7. L.V. Gribov, E.M. Levin, M.G. Ryskin: Nucl. Phys. B**188**, 555 (1981)
8. J. Bartels: TH. 3153-CERN (1981). Talk
9. V.N. Gribov, L.N. Lipatov: Sov. J. Nucl. Phys. **15**, 438, 675 (1972)
10. A.H. Mueller: Phys. Lett. B**104**, 161 (1981)
11. A. Bassetto, M. Ciafaloni, G. Maschesini, A.H. Mueller: University of Florence Preprint 82/11
12. J. Bartels, T. Jaroszewicz: in preparation
13. J. Bartels: Nucl. Phys. B**151**, 293 (1979)
14. J. Bartels: Nucl. Phys. B**175**, 365 (1980)
15. T. Jaroszewicz, J. Kwieciński: Z. Phys. C - Particles and Fields **12**, 167 (1982)
16. G. Altarelli, G. Parisi: Nucl. Phys. B**126**, 298 (1977)
17. A.A. Anselm: Leningrad Winter School 37 (1972)
18. J.D. Bjorken: In: Current induced reactions. International Summer Institute Hamburg, p. 93 (1975). Eds. J.G. Körner, G. Kramer, D. Schildknecht. Lecture Notes in Physics 56. Berlin, Heidelberg, New York: Springer 1976